Engineering and Technology Journal
Journal homepage: https://etj.uotechnology.edu.iq

Tribological properties evaluation of powdered pentaclethra macrophylla pod and gum-arabic for brake pad

I. C. C. Iloabachie[a]*, A. M. Nwankwo[b], C. C. Ogbu[c]

[a]Department of Mechanical Engineering, University of Agriculture and Environmental Sciences, Umuagwo, Imo state, Nigeria.
[b]Works and Engineering Services, Federal Polytechnic, Oko. Anambra State, Nigeria.
[c]Department of Mechanical Engineering, Institute of Management and Technology, Enugu, Nigeria.
*Corresponding author Email: yficic@gmail.com

HIGHLIGHTS

- The study introduced a novel, cost-effective approach for producing quality asbestos-free brake pads.
- Pentaclethra Macrophylla pod was used as a local reinforcement in asbestos-free brake pad production.
- Carbonization was applied as a surface modification to improve the flame resistance of the brake pad.
- Particle size and surface treatment of reinforcement affected wear resistance and friction coefficient.

Keywords:

Pentaclethra macrophylla pod
Wear rate
Flame resistance
Coefficient of friction
Carbonization

ABSTRACT

This study evaluated the tribological properties of an eco-friendly brake pad. Pentaclethra macrophylla pod was pulverized into powder form and sieved. Two particle sizes of 150 µm and 210 µm were obtained after sieving, and the sieved particles were divided into two portions, with one portion carbonized and the other uncarbonized. The brake pad composite was produced by varying the composition of powdered reinforcement in the order of 10, 20, 30, 40, and 50 wt.%. The formulation was poured into a metal mould 50 × 50 × 8 mm^3, placed in a hot platen press at a temperature of about 180 °C, a molding pressure of 15 MPa, and a curing time of 5 minutes. Post-heat treatment of the composites was performed in a hot air oven for a period of 4 hours at 180 °C. The produced brake pads were evaluated for wear rate, coefficient of friction, and flame resistance. The results showed that the coefficient of friction and flame resistance of the brake pads increased as the weight percentage composition of the powdered reinforcement increased, while the wear rate decreased. The 150 µm particle size of the powdered reinforcement recorded higher coefficient of friction values and lower wear rate. The carbonized powdered reinforcement had better resistance to the flame test. Wear rate value of 3.19 mg/m, coefficient of friction value of 0.3-0.4, and flame resistance of about 8.2% showed that powdered reinforcement is a promising reinforcement material for the production of eco-friendly brake pads.

1. Introduction

In recent times, the dominance of composite materials among the emerging engineering materials has continued to attract the interest of researchers globally like [1]. This emerging trend, which Rajan [2], hinted at, has led to a steady increase in the volume and number of applications of composite materials across various markets. Selection and application of advanced materials like these composites as friction materials for automobile brake pad production, as was noted by Maleque et al. [3], have the potential to perform better under severe service conditions like higher speed, higher load, etc., which are increasingly being encountered in modern automobiles. As was noted by Bashar et al. [4], the primary function of an automobile brake pad is to transform the kinetic energy of a vehicle to heat energy via friction and, in the process, eject the heat to the surrounding environment. Drum (shoe) brake and disk (pad) brake, Bashar et al. [4], further stated, are the major types of friction brakes. Brake friction materials observed by Sugozu et al. [5], are composites composed of several basic functional parts such as abrasives, lubricants, space fillers, fiber or pulp reinforcements, and polymer binders. Abrasives, Sugozu et al. [5], continued are added to the automobile brake pad composite formulation to increase the friction coefficient and to keep its value stable at higher temperatures. Generally, Kapoor and Sanjeev [6], reported that the formulation of every composite friction material for brake pad production has its own unique frictional behaviors and wear-resistance characteristics. As was reported by Idris et al., [7].

Idris et al. [7], brake pads generally consist of asbestos embedded in the polymeric matrix, among other ingredients. However, the use of asbestos in automobile brake pad formulation, as countered by Ikpambese et al. [8], is being avoided due to

http://doi.org/10.30684/etj.2025.157355.1900
Received 04 August 2025; Received in revised form 05 September 2025; Accepted 06 September 2025; Available online 20 October 2025
2412-0758/University of Technology-Iraq, Baghdad, Iraq

its carcinogenic and harmful nature; hence, new asbestos-free materials and brake pads have been developed. Therefore, environmental regulations and ethical concerns have prompted the search for environmentally friendly materials.

Agricultural residues or wastes like shells of various dry fruits, rice husks, wheat husk, straws, and hemp fiber now serve as emerging eco-friendly new and inexpensive materials in the development of brake pads with commercial viability and environmental acceptability. Aigbodion and Agunsoye [9], reported the development of an asbestos-free brake pad using sugar cane bagasse. Ibhadode and Dagwa [10], also developed asbestos-free friction lining materials using palm kernel shell. Idris et al. [7], produced eco-friendly asbestos-free brake pads using banana peels, and the findings concluded that banana peels can be effectively used to replace asbestos. Ruzaidi et al. [11], developed an asbestos-free brake pad using palm slag, and the results indicated that palm slag can be used effectively as an alternative to asbestos in brake pad production. Mathur et al. [12], evaluated the hardness and tribological behaviour of non-asbestos brake lining materials for automobiles using cashew nut shell liquid modified phenolic resin as a binder, graphite or cashew dust as a friction modifier, and barium sulphate, talc, and wollastonite as fillers. They established that the hardness of friction materials plays a crucial role in the evaluation of tribo-performance of brake pads and can be controlled by suitable modifications in the composition of the composite material.

Maleque et al. [13], developed a new natural fibre reinforced aluminium composite for automotive brake pad application using varying coconut fibre contents in phenolic resin binder. They reported better properties in terms of higher density, lower porosity, and higher compressive strength for 5 and 10% coconut fiber compositions. They concluded that 5 and 10% showed better physico-mechanical properties compared to other formulations. Ikpambese et al. [8], evaluated palm kernel fibers (PKFs) for the production of asbestos-free automotive brake pads using epoxy resin binder. The resin binder and the palm kernel fibers were varied in composition. Ikpambese et al. [8] reported that the wear rate, coefficient of friction, noise level, temperature, and stopping time of the produced brake pads increased with increasing speed and attained better properties at a composition of 40% epoxy-resin, 10% palm wastes, 6% Al_2O_3, 29% graphite, and 15% calcium carbonate. Lawal et al. [14], investigated the development and production of brake pads using sawdust and epoxy resin by compression molding. They established that the finer the sieve size, the better the investigated properties, like microstructure analysis, hardness, compressive strength, density, ash content, wear rate, and water absorption. Lawal et al. [14], concluded that sawdust of 100 µm particle size has properties that can effectively replace asbestos in brake pad manufacture, since it gives better brake pad properties. Most of the developed brake pads using agro waste materials, when compared with premium asbestos-based commercial brake pads, offered satisfactory performance. The reviewed works did not consider Pentaclethra macrophylla pod as an alternative reinforcement material for brake pad production. Also, Pentaclethra macrophylla pod and gum Arabic resin are natural plant-based materials likely to be more environmentally friendly than synthetic materials.

Pentaclethra macrophylla pod is a waste material that litters the environment after the splitting of the pod to release the seed. It constitutes an environmental eyesore; hence, the need to find an alternative application for its consumption that will be environmentally friendly. This work, therefore, centered on exploring the potential of a powdered Pentaclethra macrophylla as an alternative friction material in gum Arabic resin for the production of an eco-friendly brake pad.

2. Materials and Methods

2.1 Materials

The primary materials utilized in this study include dry ground Pentaclethra Macrophylla pods, sourced from Adu-Achi, Oji River Local Government Area, Obiagu-Otuku in Enugu East Local Government Area, and Agbani in Nkanu West Local Government Area, all within Enugu State, South-East, Nigeria. Grade 1 Gum-Arabic resin sourced from Gombe State in Northern Nigeria was employed as a binder. Grade 1Gum-Arabic resin exhibits good thermal properties, decomposing at higher temperatures. Between 30 and 170 °C, grade 1Gum-Arabic resin loses 9 to 9.62% of its water, which is basically due to elimination of its surface and structural water. Denaturation of polysaccharides and the decomposition of carboxylate groups and carboxylic acids in grade 1Gum-Arabic resin occur around 170 to 400 °C, which results in significant weight loss of over 55%. Other essential components incorporated were eggshell powder as filler, waste car tire particles functioning as a friction modifier, and graphite serving as a lubricant, as showen in Figure 1.

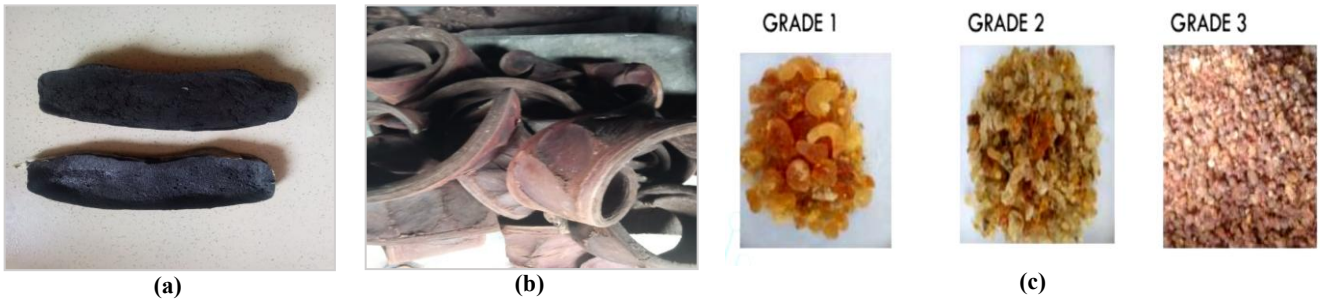

Figure 1: a) Produced brake pad using powdered pentaclethra macrophylla pod in Gum-Arabic resin, b) Pentaclethra Macrophylla pod, c) Grades of Nigerian Gum-Arabic

2.2 Methods

2.2.1 Raw material collection and processing

The dry Pentaclethra macrophylla pods were manually gathered from the wild, ensuring they were free from unwanted particles. They were then washed thoroughly with distilled water and left to dry in the sun for approximately six hours. To remove residual moisture, the pods were subjected to oven drying at 110 °C for three hours until a stable weight was achieved, followed by cooling. The dried pods were subsequently crushed into fine powder using a locally fabricated grinding machine. The ground material was then sieved using a set of sieves arranged in descending order of mesh size, in line with ASTM E11/ISO 3310 standard. The resultant powder was split into two portions: one was carbonized, and the other remained uncarbonized.

The carbonization process involved packing the dry powdered Pentaclethra macrophylla pods in an earthen pot, covered with a lid, and heated in an inert atmosphere in an electric resistance furnace model KGVB Kohaszat Gyarepito Vallalat, type Koo 80/50-120 Temperature -950 °C 513-4124 -0730/B at temperatures of about 950 °C with a heating rate of about 10 °C per minute and a soaking time of about three hours.

2.2.2 Preparation of composite samples

The study involved varying the proportions of powdered Pentaclethra Macrophylla pods and gum arabic resin, while keeping the amounts of the lubricant, friction modifier, and abrasives unchanged. The reinforcement, along with the waste car tire particles, graphite, eggshell powder, and silica abrasives, was mixed thoroughly in a separate container before being combined with the resin. The mixture was then poured into a locally fabricated mixer (100 to 500 rpm) and stirred for about ten minutes to achieve uniformity. The proportion of Pentaclethra macrophylla powder was adjusted to 10, 20, 30, 40 and 50 wt.%. This mixture was then poured into a metal mold (50 × 50 × 8 mm^3) and subjected to hot compression molding at 180 °C under a pressure of 15 MPa for five minutes. To enhance the structural integrity of the composite, post-curing was performed in a hot air oven at 180 ℃ for four hours. Table 1 shows the constituents of the mixture and their percentage compositions.

Table 1: Composite sample mixture

S/N	Constituents	Percentage compositions (%)				
		1	**2**	**3**	**4**	**5**
1	Matrix(Gum Arabic Grade 1)	60	50	40	30	20
2	Reinforcements (PM)	10	20	30	40	50
3	Filler (Egg Shell)	10	10	10	10	10
4	Catalyst (MEKP)	0.5	0.5	0.5	0.5	0.5
	Accelerator (Cobalt naphthenate)	0.5	0.5	0.5	0.5	0.5
5	Abrasives (CaO)	5	5	5	5	5
6	Abrasives (SiO_2)	5	5	5	5	5
7	Friction Modifiers (Graphite)	9	9	9	9	9
	Total	100	100	100	100	100

2.2.3 Wear rate measurement

The wear rate was examined using a pin-on-disc apparatus, in compliance with the ASTM G 99 standard. A gray cast iron disc with a diameter of 180 mm and a thickness of 8 mm was utilized. The initial weight of each sample was recorded using a precision electronic balance with an accuracy of 0.0001 g. The specimen was then securely positioned on the tribometer, pressing against the rotating disc with a surface roughness of 0.3 µm, under an applied load of 20 N, a sliding speed of 5.02 m/s, and a total sliding distance of 5 km. The difference in weight before and after testing was used to determine material loss. The wear rate was calculated using Equation 1:

$$\text{Wear Rate} = \frac{\Delta W}{s} \quad (1)$$

where ΔW represents the weight loss, and S is the sliding distance in meters.

2.2.4 Coefficient of friction measurement

The coefficient of friction was determined using an inclined plane setup and a 90° wedge. The test sample was positioned on the inclined plane, and the wedge angle was gradually adjusted until the specimen began to slide. This provided an estimate of the static friction coefficient.

2.2.5 Flame resistance evaluation

Flame resistance is the term used to describe a material that burns slowly or is self-extinguishing after the removal of an external source of ignition. This was assessed by exposing the composite specimens to direct heat using a Bunsen burner. The samples were placed on wire gauze directly over the blue flame and subjected to heating for ten minutes. The weight of each sample was recorded before and after the test to evaluate the extent of degradation due to combustion, using Equation 2:

$$\frac{\text{Wcbc} - \text{Wcac}}{\text{Wcbc}} \times 100 = \text{Mass retained} \quad (2)$$

where Wcbc is the weight of the composite before combustion, and Wcac is the weight of the composite after combustion.

3. Results and discussion

In the analysis of the carbonized and uncarbonized, an SEM /EDX imaging was done for the samples. The element name, symbol and numbers are clearly shown in a and in b the disabled element is shown. Also with the atomic concentration and weight concentration. In Figure 2 (a and b) is for the uncarbonized developbed at 40 wt.% @ 150 µm Wear was taken at 17.11 hours and Figure 3 (a and b) show the carbonized developed 30 wt.% @ 210 µm Wear taken at 17.21 hours, and Figure 4 (a and b) shows another uncarbonized taken 16.14 hours developed for 20 wt.% @ 210 µm Wear.

From Figure 5, it could be observed that the coefficient of friction of the developed brake pad increased as the weight percent of the powdered Pentaclethra Macrophylla pod increased, and this agreed with the work of [15]. This may be likened to the appearance of significant plastic deformation on the pin disc surface in line with [16]. In terms of surface modification, the carbonized powdered Pentaclethra Macrophylla pod reinforced Gum-Arabic brake pad sample had the lowest value of the coefficient of friction. A higher value of the coefficient of friction was recorded in the un-carbonized sample.

Also, the lower particle size of 150 µm had the highest coefficient of friction value compared to the 210 µm particle size. The 0.3 to 0.4 value of the coefficient of friction obtained in this work is within the range reported by Ibhadode et al., [10]. In Figure 5, it could be observed that the wear rate of the developed brake pad decreased as the percentage composition of the reinforcement increased from 10 to 30 wt.%. This trend was, however, reversed when the reinforcement particles increased from 40 to 50 wt.%. A similar trend had been reported by Aigbodion [17], where maize husk acted both as a friction and abrasion-resistant material in epoxy resin. The decreased wear rate of the developed brake pad may be a result of the higher load-bearing capacity of the developed brake pad composite and better interfacial bonding between the reinforcement particles and the resin used in this work, thereby reducing the possibility of particle pull-out from the resin, which may result in higher wear state by Tudu [18]. In addition, the developed brake pad samples containing 150 µm particle size of the reinforcement recorded the least wear rate values compared to the 210 µm particle size reinforced brake pad. This may be viewed as a closer packing of the particles in the resins as the particle size decreased, leading to a stronger bond between the resins and the powdered Pentaclethra macrophylla Pod. The carbonized powdered Pentaclethra macrophylla pod reinforced brake pads mostly had lower wear rate values compared to the un-carbonized samples. This, however, contradicts the work of Idris [7], where un-carbonized banana peels brake pads had a lower wear rate than the carbonized ones. This variation may be likened to the grade of gum Arabic resin used in this work.

The flame resistance of the produced brake pads, as can be seen in Figure 6, increased as the reinforcement weight percent increased. This is in line with the works of [10]. It could be suggested that proper bonding between the powdered Pentaclethra Macrophylla pod and the resin accounted for this.

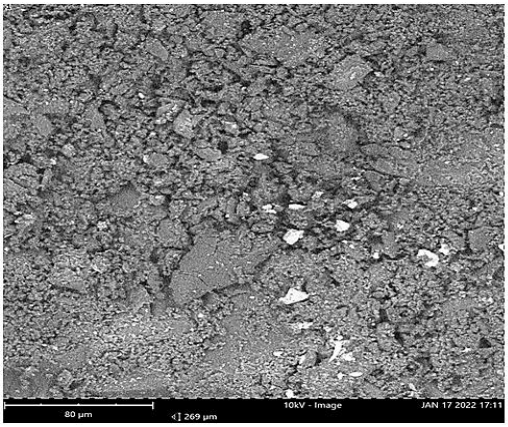

Element Number	Element Symbol	Element Name	Atomic Conc.	Weight Conc.
6	C	Carbon	72.29	66.20
8	O	Oxygen	27.71	33.80

(a)

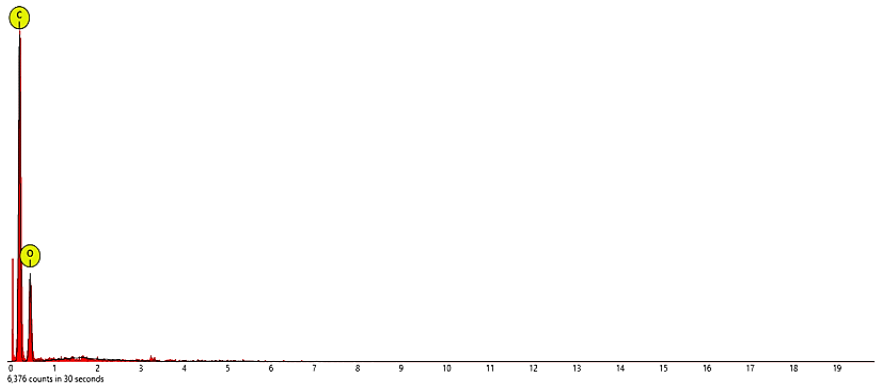

(b)

Figure 2: SEM/EDX of Developed 40 wt.% Un-carbonized @ 150 µm Wear a) FOV: 269 µm, Mode: 10kV - Image, Detector: BSD Full, Time: JAN 17 2022 17:11, and b) Disabled elements

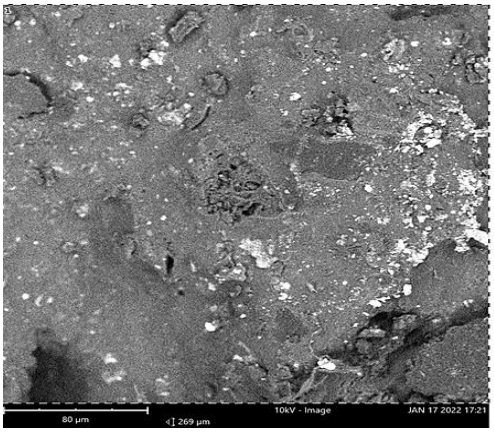

Element Number	Element Symbol	Element Name	Atomic Conc.	Weight Conc.
6	C	Carbon	61.57	54.60
8	O	Oxygen	38.43	45.40

(a)

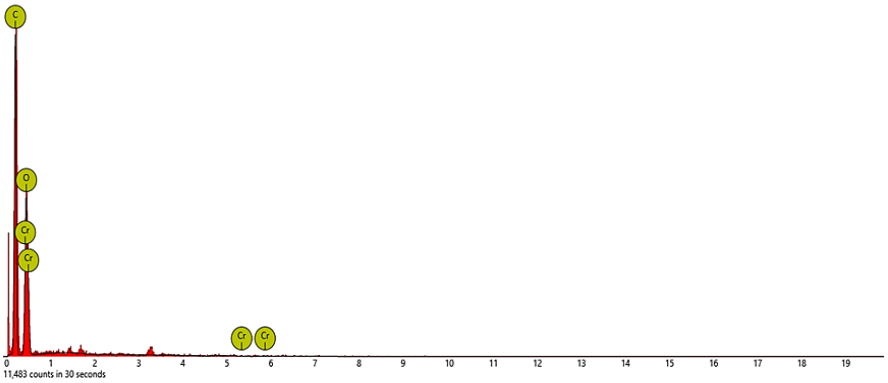

(b)

Figure 3: SEM/EDX of Developed 30 wt.% Carbonized @ 210 µm Wear a) FOV: 269 µm, Mode: 10kV - Image, Detector: BSD Full, Time: JAN 17 2022 17:21, and b) Disabled elements

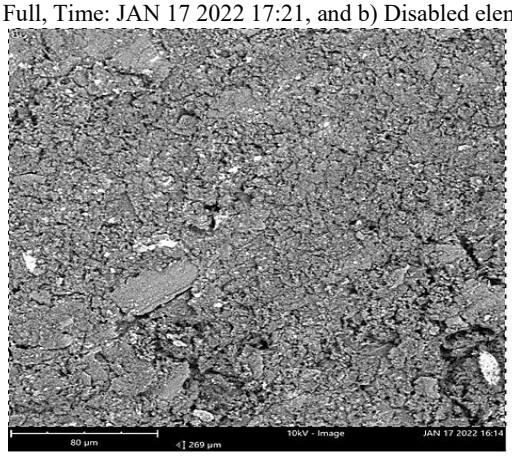

Element Number	Element Symbol	Element Name	Atomic Conc.	Weight Conc.
6	C	Carbon	79.91	74.91
8	O	Oxygen	20.09	25.09

(a)

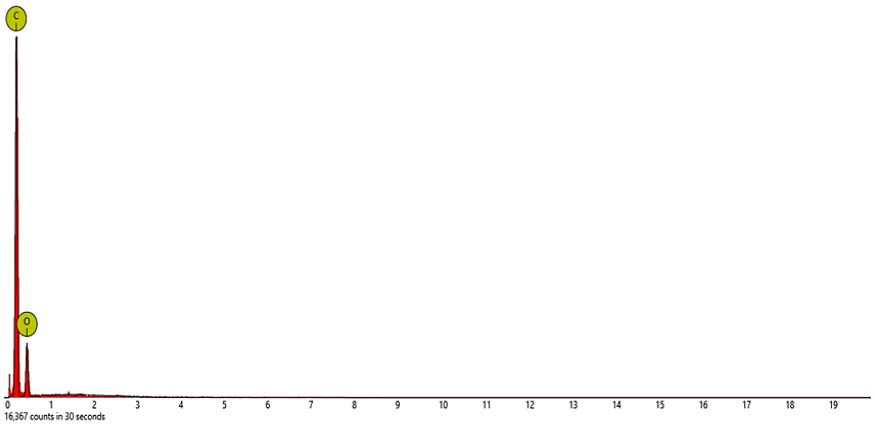

(b)

Figure 4: SEM/EDX of Developed 20wt. % Un-Carbonized @ 210 µm Wear a) FOV: 269 µm, Mode: 10kV - Image, Detector: BSD Full, Time: JAN 17 2022 16:14, and b) Disabled elements

Also, the developed brake pad reinforced with the powdered carbonized Pentaclethra Macrophylla pod had higher flame resistance compared to the un-carbonized brake pad samples, and agrees with the work of Idris et al. [7], where a similar trend was established. This is an indication that carbonization of the Pentaclethra Macrophylla pod leads to enhancement of the thermal stability of the developed brake pad. The 150 µm particle size of the reinforced developed brake pad had better flame resistance property than the 210 µm particle size reinforced brak pad sample. It may be likened to increased pores as the particle size of the reinforcement increases. Aigbodion et al. [9], established a similar trend.

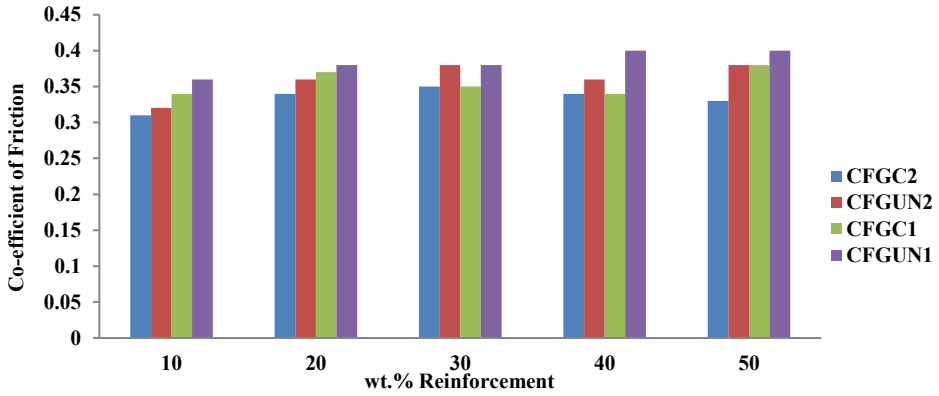

Figure 5: Effect of surface modification, particle size and wt.% on the coefficient of friction of gum-arabic resin/powdered pentaclethra macrophylla based brake pad composite

KEY: CFGC2-Coefficient of Friction Gum Arabic resin Carbonized with 210 µm reinforcement particle size, CFGUN1-Coefficient of Friction Gum Arabic resin Un-carbonized with 150 µm reinforcement particle size.

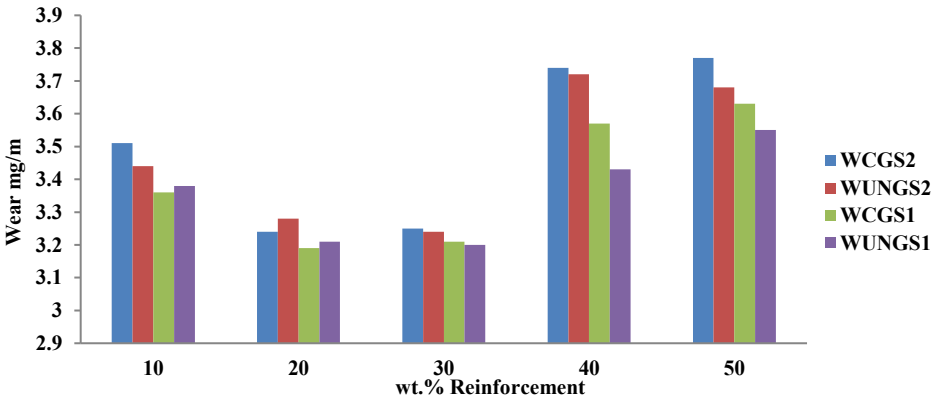

Figure 6: Effect of surface modification, particle size and wt.% on the wear rate of gum-arabic resin/powdered pentaclethra macrophylla based brake pad composite

KEY: WCGS2: Wear Carbonized Gum Arabic Sample with 210 µm reinforcement particle size, WUNGS1: Wear Un-Carbonized Gum Arabic Sample with 150 µm reinforcement particle size.

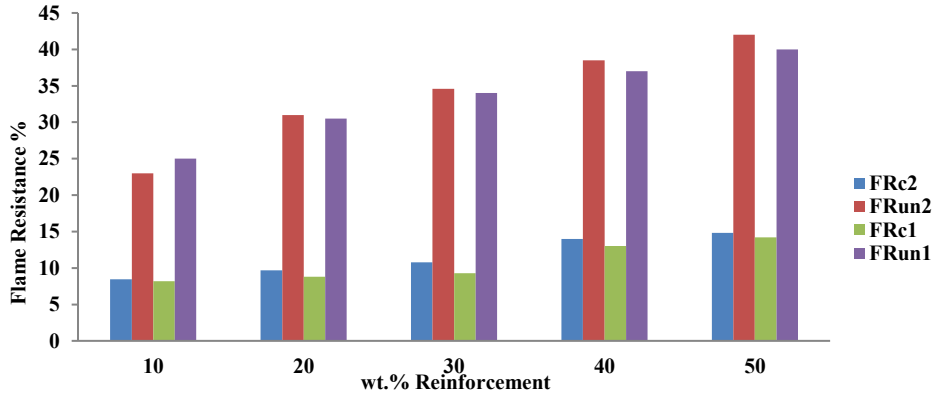

Figure 7: Effect of surface modification, particle size and wt.% on the flame resistance (%) value of gum-arabic resin/powdered pentaclethra macrophylla pod-based brake pad composite

KEY: FRc2-Flame Resistance Carbonized with 210 µm reinforcement particle size, FRun1-Flame Resistance Uncarbonized with 150 µm reinforcement particle size.

3.1 Variation of speed with coefficient of friction

The effect of variation of speed with the coefficient of friction of the produced brake pad and commercial brake pad is presented in Figures 8 and 9. The trend of the graphs showed that generally, the coefficient of friction of the developed brake pad and commercial brake pad decreased as the speed increased. S1 to S5 showed developed brake pads using Powdered Pentaclethra Macrophylla Pod, while S6 represented a commercial brake pad. Both the developed and commercial brake pads exhibited the same trend and agreed with the work of [19]. The decrease in the coefficient of friction as the speed increased may be viewed as developed plastic deformation on the pin disc surface and is in line with the observation of [20].

However, despite the observed decrease of the coefficient of friction with speed increase, it could also be stated that there were some stable portions in the graphs where the coefficient of friction was a bit constant with increase in speed, as can be seen in the Figures 10 and 11. Ikpambese et al. [8], made similar observation and this may be attributed to non-inclusion of steel fibers in the brake pad composition which helps to increase coefficient of friction due to adherence of the steel chips to the surface of the pin disc Also, certain metal oxides like CaO and K_2O contained in the powdered Pentaclethra Macrophylla pod have lubricating effects and may have assisted the lubricant additive in the brake pad formulation to reduce further and stabilize the coefficient of friction.

The surface modification of the Pentaclethra Macrophylla pod was observed to have affected the coefficient of friction as the speed varied. The brake pad formulations with carbonized powder Pentaclethra Macrophylla pod had lower coefficient of friction values compared to the un-carbonized samples. Idris et al. [7], reported a similar trend in carbonized and uncarbonized banana peels. This may likely be as a result of carbonization of the powder Pentaclethra Macrophylla pod, which enhanced the structural strength of the pod and also improved its bond strength with the resins.

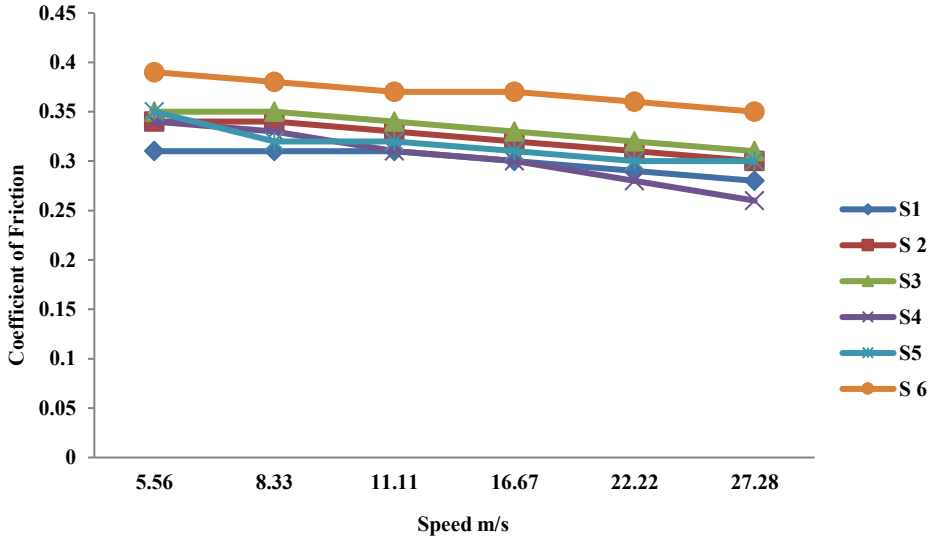

Figure 8: Effect of Speed Variation on the Coefficient of Friction for Carbonized @ 210 µm

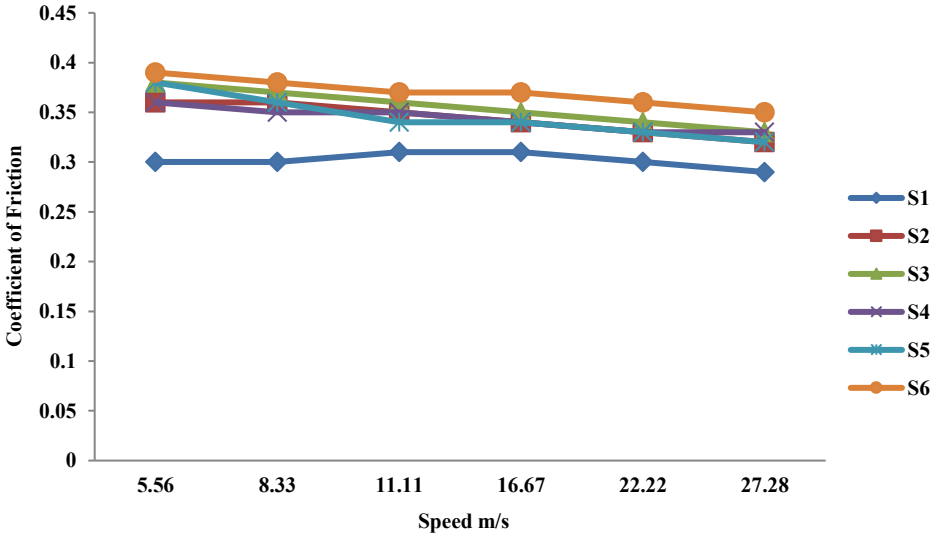

Figure 9: Effect of Speed Variation on the Coefficient of Friction for Un-carbonized @ 210 µm

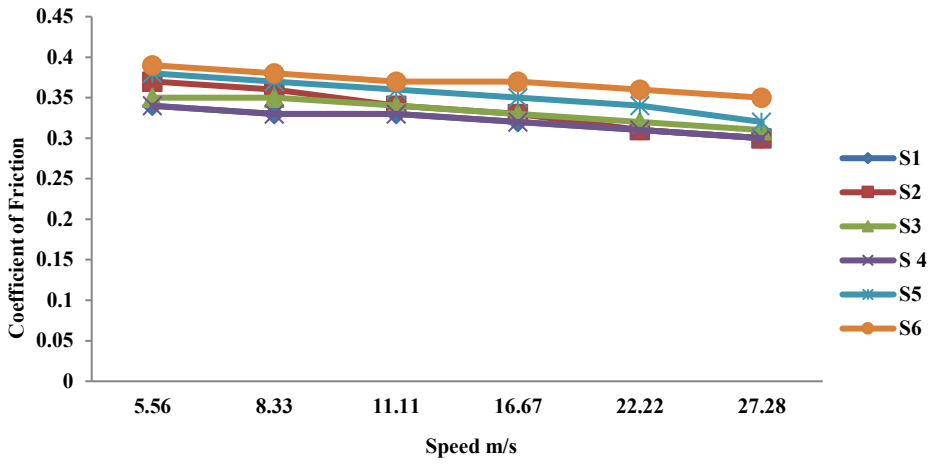

Figure 10: Effect of Speed Variation on the Coefficient of Friction for Carbonized @150 µm

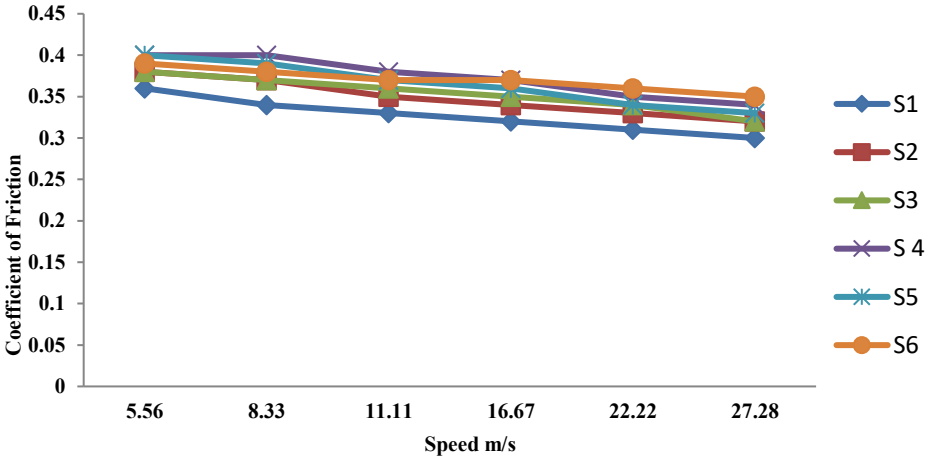

Figure 11: Effect of Speed Variation on the Coefficient of Friction for Un-carbonized @ 150 µm

KEY: S1- Developed brake pad with 10 wt.% reinforcement, S2 - Developed brake pad with 20 wt.% reinforcement, S3 - Developed brake pad with 30 wt% reinforcement, S4 - Developed brake pad with 40 wt.% reinforcement, S5 - Developed brake pad with 50 wt.% reinforcement, S6 – Commercial brake pad bought from the market.

3.2 Analysis of the modeled results

The model statistics summary table, Table 2, gives some important information about the mode for the coefficient of friction. It shows four important statistics that describe the model. These are S-value, R-squared, adjusted R-squared, and predicted R-squared. S represents the standard deviation of the distance between the data values and the fitted values. It is used to assess how well the model describes the response. The lower the value of S, the better the model; for all four responses, the value of S is sufficiently low, and this indicates that the model describes the responses appropriately.

The R-squared is the percentage of variation in the response that the model explains. The higher the R^2 value, the better the model fits the data. The adjusted R^2 is the percentage of the variation in the response that the model explains, adjusted for the number of predictors in the model relative to the number of observations. The adjusted R-squared value should be close to the R-squared value.

Table 2: Model summary statistics for coefficient of friction

S	R-sq	R-sq(adj)	PRESS	R-sq(pred)	AICc	BIC
0.0150060	97.44%	96.39%	0.0067971	91.36%	-95.01	-97.38

From Table 2, it can be seen that the values for R-squared, R-squared adjusted, and R-squared predicted for the coefficient of friction response surface design model are 0.9744, 0.9639, and 0.9136, respectively. The independent variables in the model and the effect of each variable were evaluated. Therefore, to evaluate the adequacy of the selected model, several appraisal techniques were used. The coefficient of determination (R^2), the adjusted determination coefficient (adjusted R^2), and the variation inflation factor (VIF) were used to assess the adequacy of the model, as has been employed by some researchers, such as [21]. The predicted R2 of 0.9136 is in reasonable agreement with the adjusted R^2 of 0.9639. Also, the difference between the

R-squared value and the adjusted R2 two is 0.0105. The difference is as suggested by the model. This, therefore, confirms the adequacy of the model.

In addition, the predicted R-squared is used to determine how well a model predicts the response for new observations. The higher the value, the better the model is in predicting an accurate response for a new observation. The predicted R2 value of 0.9136 is high enough to indicate the good ability to predict and also reasonably close to the R-squared value to indicate that the model is not over-fit.

The Pareto chart of Figure 12 shows the absolute values of the standardized effects from the largest effect to the smallest effect. The standardized effects are t-statistics that test the null hypothesis that the effect is 0. The chart also plots a reference line to indicate which effects are statistically significant. From Figure 12, the reference line is 1.523. On the Pareto chart of Figure 12, bars that cross the reference line are statistically significant. As shown in Figure 12, all the terms are statistically significant. The Pareto chart is also used to determine the magnitude and the importance of the effects.

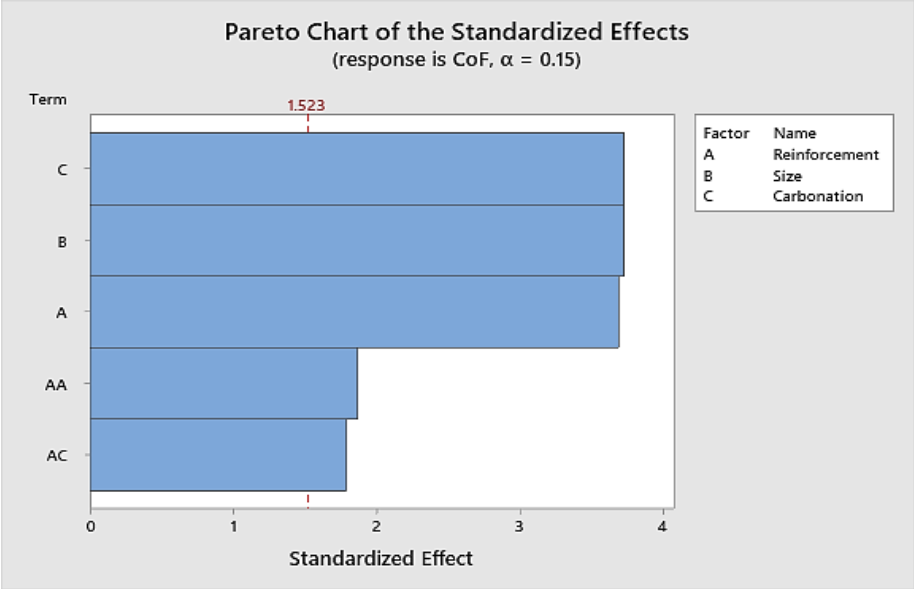

Figure 12: Pareto chart of coefficient of friction of developed powdered pentaclethra macrophylla pod/gum-arabic resin-based brake pad composite

The model for the coefficient of friction generated four residual plots. These are: Normal plot of residuals, Histogram of residuals, Residuals versus fits, and Residuals versus order, Figure 13. The points on the normal plot should generally form a straight line if the residuals are normally distributed. If the points on the plot depart from a straight line, the normality assumption may be invalid. The points in this plot for the coefficient of friction response formed a straight line; hence, it can be said that the normality assumption is valid. Furthermore, the histogram of residuals plot usually resembles a normal (bell-shaped) distribution with a mean of zero. Substantial clusters of points away from zero may indicate that factors other than those in the model may be influencing the result. There was no substantial cluster in the histogram of residuals plot for the coefficient of friction response; therefore, it is safe to say that no factor other than those in the model is influencing the result.

Nevertheless, the top - Residuals versus fits plot should show a random pattern of residuals on both sides of 0. There should not be any recognizable patterns in the residual plot. The residual versus fits plots for the coefficient of friction response showed no pattern, so the constant variance assumption is valid. The bottom - Residual versus order plot of the coefficient of friction residual is in the order that the data was collected and can be used to find non-random error, especially of time-related effects. The lack of pattern in this plot for the coefficient of friction response showed that the independence assumption is valid. Contour plots display the 3-dimensional relationship in two dimensions, with x- and y-factors (predictors, i.e., particle size of the powdered Pentaclethra Macrophylla pod on the y-axis and percentage composition of the reinforcement on the x-axis) plotted on the x- and y-scales and response values, i.e., coefficient of friction represented by contours, Figure 14 a and b. A contour plot is like a topographical map in which x-, y-, and z-values are plotted instead of longitude, latitude, and elevation. The darker regions of the contour identify higher coefficient of friction values.

Figure 14 a and b represent the carbonized and un-carbonized forms of the powdered Pentaclethra Macrophylla pod reinforcement in the brake pad formulation.

3D surface plots are used to explore the potential relationship between three variables. Figure 15 a and b showed the 3D surface plots of the carbonized and un-carbonized powdered Pentaclethra Macrophylla pod reinforcement in gum-arabic resin brake pad formulation. The predictor variables, i.e., particle size of the powdered Pentaclethra Macrophylla pod on the y-axis and percentage composition of the reinforcement on the x-axis, are displayed on the x- and y-scales, and the response (z) variable, coefficient of friction, is represented by a smooth surface (3D surface plot).

From Figure 15 a and b, it can be observed that the 150 µm particle size of the reinforcement had a higher coefficient of friction value than the 210 µm particle size of the reinforcement in both the carbonized and un-carbonized samples of the developed brake pad samples.

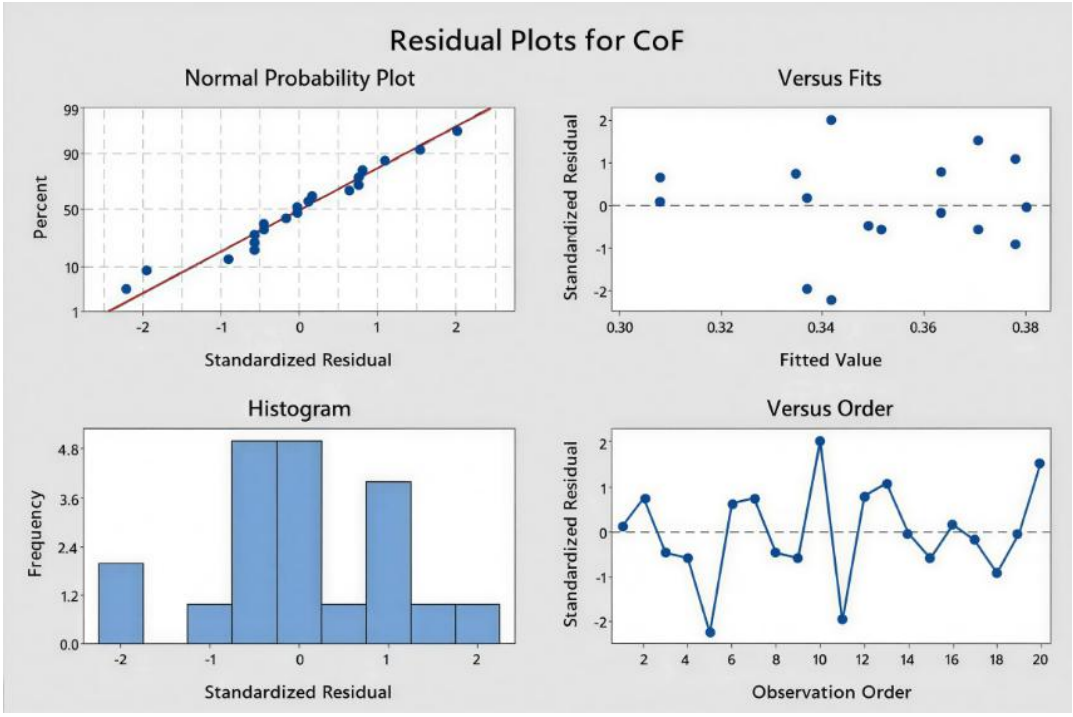

Figure 13: Residual plots for coefficient of friction of developed powdered pentaclethra macrophylla pod / gum-arabic resin-based brake pad composite

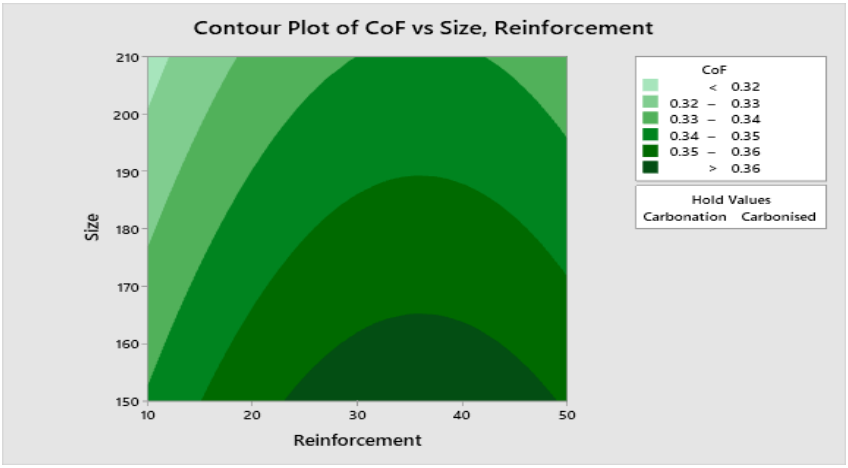

(a)

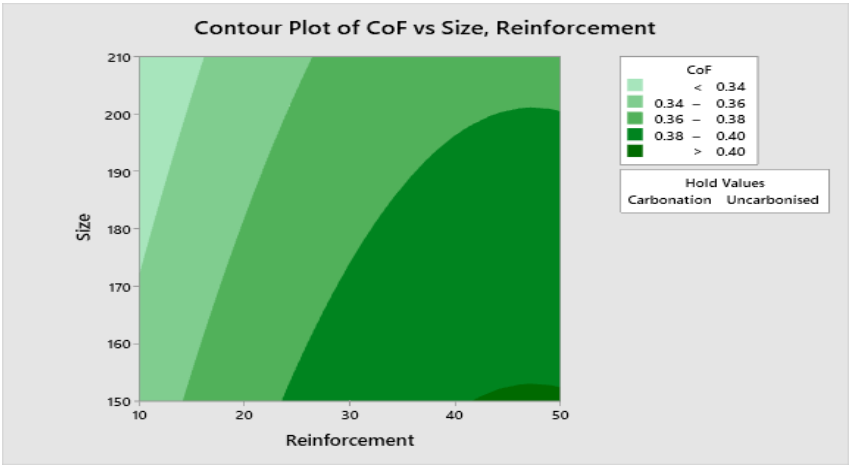

(b)

Figure 14: a) Contour plots for coefficient of friction of carbonized developed powdered pentaclethra macrophylla pod / gum-arabic resin-based brake pad composite, b) contour plots for coefficient of friction of un-carbonized developed powdered pentaclethra macrophylla pod / gum-arabic resin based brake pad composite

The model statistics summary table, Table 3, gives some important information about the model for flame resistance. It shows four important statistics that describe the model for flame resistance. These are S-value, R-squared, adjusted R-squared, and predicted R-squared. S represents the standard deviation of the distance between the data values and the fitted values. It is used to assess how well the model describes the response. The lower the value of S, the better the model; for all four responses, the value of S is sufficiently low, and this indicates that the model describes the responses appropriately.

The R-squared is the percentage of variation in the response that the model explains. The higher the R^2 value, the better the model fits the data. The adjusted R^2 is the percentage of the variation in the response that the model explains, adjusted for the number of predictors in the model relative to the number of observations. The adjusted R-squared value should be close to the R-squared value.

Table 3: Model summary statistics for flame resistance

S	R-sq	R-sq(adj)	PRESS	R-sq(pred)	AICc	BIC
1.14396	99.29%	99.15%	34.5887	98.82%	71.96	72.65

From Table 3, it can be seen that the values for R-squared, R-squared adjusted, and R-squared predicted for the flame resistance response surface design model are 0.9929, 0.9915, and 0.9882, respectively. The independent variables in the model and the effect of each variable were evaluated. Therefore, to evaluate the adequacy of the selected model, several appraisal techniques were used. The coefficient of determination (R^2), the adjusted determination coefficient (adjusted R^2), and the variation inflation factor (VIF) were used to weigh the adequacy of the model, as has been used by some researchers [19]. The predicted R^2 of 0.9882 is in reasonable agreement with the adjusted R^2 of 0.9915. Also, the difference between the R-squared value and the adjusted R^2 two is 0.0014. The difference is as suggested by the model. This, therefore, confirms the adequacy of the model. In addition, the predicted R-squared is used to determine how well a model predicts the response for new observations. The higher the value, the better the model is in predicting an accurate response for a new observation. The predicted R^2 value of 0.9882 is high enough to indicate good ability to predict and also reasonably close to the R-squared value to indicate that the model is not over-fit.

The Pareto chart of Figure 16 shows the absolute values of the standardized effects from the largest effect to the smallest effect. The standardized effects are t-statistics that test the null hypothesis that the effect is 0. The chart also plots a reference line to indicate which effects are statistically significant. From Figure 16, the reference line is 1.51. On the Pareto chart of Figure 16, bars that cross the reference line are statistically significant. As shown in Figure 16, all terms are statistically significant. The Pareto chart is also used to determine the magnitude and the importance of the effects.

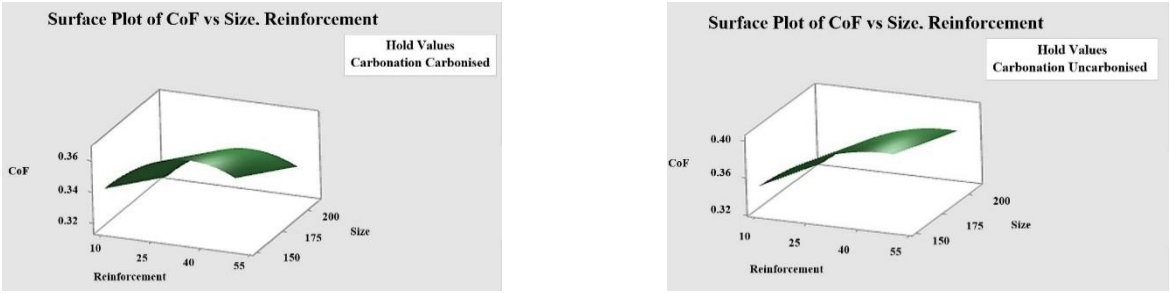

(a) **(b)**

Figure 15: a) Surface plots (3-D) for the coefficient of friction of carbonized, b) surface plots (3-D) for coefficient of friction of un-carbonized

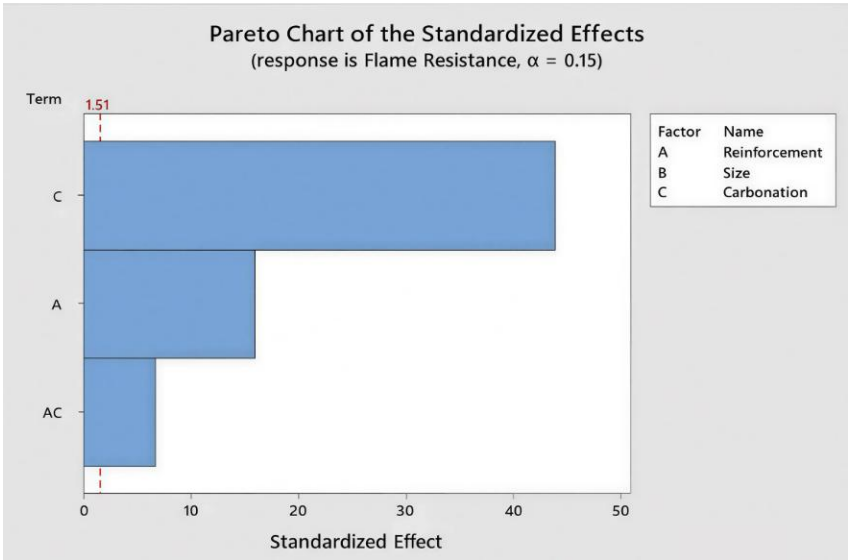

Figure 16: Pareto chart of developed powdered pentaclethra macrophylla pod / gum-arabic based brake pad composite

The model for flame resistance generated four residual plots. These are: Normal plot of residuals, Histogram of residuals, Residuals versus fits, and Residuals versus order, Figure 17. The points on the normal plot should generally form a straight line if the residuals are normally distributed. If the points on the plot depart from a straight line, the normality assumption may be invalid. The points in this plot for flame resistance response formed a straight line; hence, it can be said that the normality assumption is valid. Furthermore, the histogram of residuals plot usually resembles a normal (bell-shaped) distribution with a mean of zero. Substantial clusters of points away from zero may indicate that factors other than those in the model may be influencing the result. There was no substantial cluster in the histogram of residuals plot for flame resistance response; therefore, it is safe to say that no factor other than those in the model is influencing the result.

Nevertheless, the Residuals versus fits plot should show a random pattern of residuals on both sides of 0. There should not be any recognizable patterns in the residual plot. The residual versus fits plots for flame resistance response showed no pattern, so the constant variance assumption is valid. The Residual versus order plot of the flame resistance residual is in the order that the data was collected and can be used to find non-random error, especially of time-related effects. The lack of pattern in this plot for the flame resistance response showed that the independence assumption is valid.

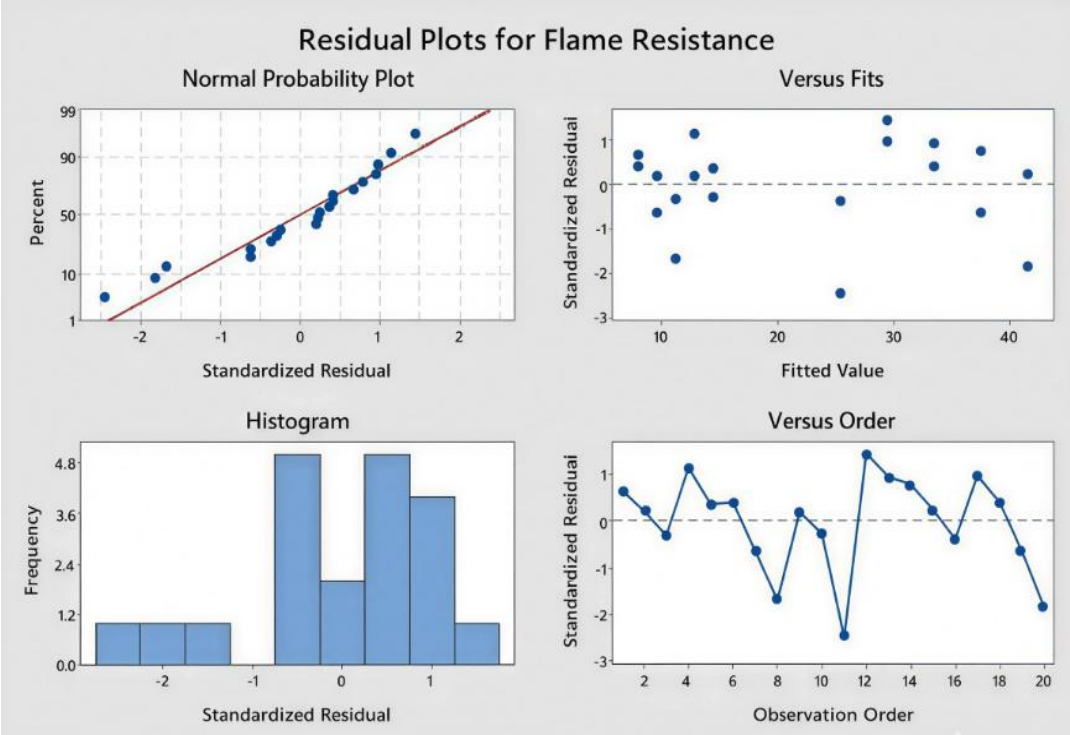

Figure 17: Residual plots of flame resistance

3.3 Response optimization

The response surface regression model uses response optimization to find the optimal values of the responses. Response optimization can minimize, maximize, or set a target for the response to optimize. Response optimization selects the optimal combination of the component amounts and the process variables required to meet the target. It can be done individually for each response, whereby the optimal factors for a single response are selected, or a multi-response optimization that tries to optimize all the responses simultaneously. Table 4 below presents the response optimization variables and their goals, targets and importamce.

Table 4: Response optimization parameters

Response	Goal	Lower	Target	Upper	Weight	Importance
Flame Resistance	Maximum	8.2%	42.00%	45.00%	1	1
CoF	Maximum	0.3	0.400	0.43	1	1
Wear Rate	Minimum	3.190 mg/m	3.770 mg/m	3.90 mg/m	1	1

4. Conclusion

A novel material - Pentaclethra macrophylla pod was studied and analyzied using empirical and numerical analysis for the production of asbestos-free brake pad. The study shows that the Powdered Pentaclethra macrophylla pod can be used as reinforcement material in the production of asbestos-free brake pads. Its surface modification processes, such as carbonization, can be used to improve the flame resistance of a brake pad. Particle size of reinforcement material for the production of, as well as its surface modification, affects the wear resistance and coefficient of friction of the produced brake pad. We conclude that Pentaclethra macrophilla pod can be a suitable substitute reinforcement for the production of automobile brake pads.

Author contributions

Conceptualization, **I. Iloabachie** and **A. Nwankwo**; data curation, **A. Nwankwo**; formal analysis, **I. Iloabachie**; investigation, **I. Iloabachie**; methodology, **I. Iloabachie** and **A. Nwankwo**; project administration, **A. Nwankwo**; resources, **C. Ogbu**; software, **I. Iloabachie** and **C. Ogbu**; supervision, **A. Nwankwo**; validation, **I. Iloabachie**., **A. Nwankwo**. and **C. Ogbu**; visualization, **I. Iloabachie**; writing—original draft preparation, **I. Iloabachie**; writing—review and editing, **I. Iloabachie**. All authors have read and agreed to the published version of the manuscript.

Funding

This research received no specific grant from any funding agency in the public, commercial, or not-for-profit sectors.

Data availability statement

The data that support the findings of this study are available on request from the corresponding author.

Conflicts of interest

The authors declare that there is no conflict of interest.

References

[1] I. C. C. Iloabachie, C. U. Atuanya, C. C. Ogbu, Optimization Analysis of Hardness Test for Powdered Pentaclethra Macrophylla Pod /Bio-Epoxy Resin-Based Brake Pad Composite Using Central Composite Design, J. Eng. Res. Rep., 24 (2023) 19–28 . http://dx.doi.org/10.9734/JERR/2023/v24i12857

[2] T. P. D. Rajan, R. M. Pillai, B. C. Pai, K. G. Satyanarayana, P. K. Rohatgi, Fabrication and Characterization of Al–7Si–0.35Mg/Fly Ash Metal Matrix Composites Processed by Different Stir Casting Routes, Compos. Sci. Technol., 67 (2007) 3369–3377. https://doi.org/10.1016/j.compscitech.2007.03.028

[3] M. A. Maleque, S. Dyuti , M. M. Rahman, Material Selection Method in Design of Automotive Brake Disc, Proceedings of the World Congress on Engineering, London, 2010.

[4] D. A. Bashar, P. B. Madakson, J. Manji, Material Selection and Production of a Cold-Worked Composite Brake Pad, World J. Eng. Pure , Appl. Sci., 2 (2012) 92–97.

[5] K. B. Sugozu, B. Daghan, A. Akdemir, N. Ataberk, Friction and Wear Properties of Friction Materials Containing Nano/Micro-Sized Sio_2 Particles, Ind. Lubr. Tribol.,68 (2016) 259–266. https://doi.org/10.1108/ILT-06-2015-0083

[6] S. Kapoor, M. Sanjeev, A Paper Review on the Scope of Non-Asbestos and Natural Waste Materials, Int. J. Adv. Eng. Res. Sci., 3 (2016) 107–112.

[7] U. D. Idris, V. S. Aigbodion, I. J. Abubakar, C. I. Nwoye, Eco-friendly asbestos-free pad: Using banana peels, J. King Saud Univ. Eng. Sci., 27 (2015) 185–192. http://dx.doi.org/10.1016/j.jksues.2013.06.006

[8] K. K. Ikpambese, D. T. Gundu, L. T. Tuleun, Evaluation of Palm Kernel Fibers (PKFs) for Production of Asbestos-Free Automotive Brake Pads, J. King Saud Univ. Eng. Sci., 28 (2014) 110–118. https://doi.org/10.1016/j.jksues.2014.02.001

[9] Aigbodion, V. S. & Agunsoye, J. O. Bagasse (Sugarcane waste): Non-Asbestos Free Brake Pad Materials; LAP Lambert Academic Publishing, Germany, 2010.

[10] A. O. A. Ibhadode, I. M. Dagwa, The Development of Asbestos–Free Friction Lining Material from Palm Kernel Shell, J. Braz. Soc. Mech. Sci. & Eng., 30 (2008)166–173. https://doi.org/10.1590/S1678-58782008000200010

[11] C. M. Ruzaidi, H. Kamarudin, J. B. Shamsul, A. M. Al Bakri, A. Alida, Morphology and Wear Properties of Palm Ash and PCB Waste Brake Pad, International Conference on Asia Agriculture and Animal IPCBEE, Singapore, 1, 2011, 145–149. http://dx.doi.org/10.13140/2.1.2659.9682

[12] R. B. Mathur, P. Thiyagarajan, T. L. Dhami, Controlling the Hardness and Tribological Behavior of Non-Asbestos Brake Lining Materials for Automobiles, J. Carbon Sci., 5 (2004) 6–11.

[13] M. A. Maleque, A. Atiqah, R.J. Talib, H. Zahurin, New Natural Fibre Reinforced Aluminium Composite for Automotive Brake Pad, Int. J. Mech. Mater. Eng.,7 (2012) 166–170.

[14] S. S. Lawal, K. C. Bala, A. T. Alegbede , Development and Production of Brake Pad from Sawdust Composite, Leonardo J. Sci., 30 (2017) 47–56.

[15] I. C. C. Iloabachie, S. M. O. Obiorah, I. C. Ezema, V. I. Henry, O. H. Chime, Effects of Carbonization on the Physical and Mechanical Properties of Coconut Shell Particle Reinforced Polyester Composite, Int. J. Res. Adv. Eng. Technol., 3 (2017) 62–69.

[16] H. Jin, Y. Wu, S. Hou, Y. Li, M. Liu, Z. Ji, J. Yuan, The Effect of Spherical Silica Powder on the Tribological Behavior of Phenolic Resin–Based Friction Materials, Tribol. Lett., 51 (2013) 65–72. https://doi.org/10.1007/s11249-013-0146-6

[17] V. S. Aigbodion, U. Akadike, S. B. Hassan, F. Asuke, J. O. Agunsoye , Development of asbestos – free brake pad using bagasse, Tribol. Ind., 32 (2010) 12–18.

[18] Tudu, P. Processing and Characterization of Natural Rubber Reinforced Polymer Composites. Bachelor's Thesis, National Institute of Technology, Rourkela, 2009.

[19] M. Kumar, J. Bijwe, Role of Different Metallic Fillers in Non-Asbestos Organic (NAO) Friction Composites for Controlling Sensitivity of Coefficient of Friction to Load and Speed, Tribol. Int., 43 (2010) 965–974. https://doi.org/10.1016/j.triboint.2009.12.062

[20] I. C. Iloabachie, B. O. Okpe, T. O. Nnamani, A. C. Chime, The Effect of Carbonization Temperatures on Proximate Analysis of Coconut Shell, Int. J. Adv. Eng. Technol., 2 (2018) 30–32.

[21] G. Chen, J. Chen, C. Srinivasakannan, J. Peng, Application of Response Surface Methodology for Optimization of the Synthesis of Synthetic Rutile from Titania Slag, Appl. Surf. Sci., 258 (2012) 3068–3073. https://doi.org/10.1016/j.apsusc.2011.11.039